

CASE REPORT OPEN

Cytogenomic identification and long-read single molecule real-time (SMRT) sequencing of a *Bardet–Biedl Syndrome 9* (*BBS9*) deletion

Jennifer Reiner^{1,4}, Laura Pisani^{1,5}, Wanqiong Qiao^{1,2}, Ram Singh^{1,2}, Yao Yang^{1,2,3}, Lisong Shi^{1,2}, Wahab A. Khan^{1,2}, Robert Sebra^{1,2,3}, Nnette Cohen^{1,6}, Arvind Babu^{1,2}, Lisa Edelmann^{1,2}, Ethylin Wang Jabs¹ and Stuart A. Scott^{1,2}

Bardet–Biedl syndrome (BBS) is a recessive disorder characterized by heterogeneous clinical manifestations, including truncal obesity, rod-cone dystrophy, renal anomalies, postaxial polydactyly, and variable developmental delays. At least 20 genes have been implicated in BBS, and all are involved in primary cilia function. We report a 1-year-old male child from Guyana with obesity, postaxial polydactyly on his right foot, hypotonia, ophthalmologic abnormalities, and developmental delay, which together indicated a clinical diagnosis of BBS. Clinical chromosomal microarray (CMA) testing and high-throughput BBS gene panel sequencing detected a homozygous 7p14.3 deletion of exons 1–4 of *BBS9* that was encompassed by a 17.5 Mb region of homozygosity at chromosome 7p14.2–p21.1. The precise breakpoints of the deletion were delineated to a 72.8 kb region in the proband and carrier parents by third-generation long-read single molecule real-time (SMRT) sequencing (Pacific Biosciences), which suggested non-homologous end joining as a likely mechanism of formation. Long-read SMRT sequencing of the deletion breakpoints also determined that the aberration included the neighboring *RP9* gene implicated in retinitis pigmentosa; however, the clinical significance of this was considered uncertain given the paucity of reported cases with unambiguous *RP9* mutations. Taken together, our study characterized a *BBS9* deletion, and the identification of this shared haplotype in the parents suggests that this pathogenic aberration may be a BBS founder mutation in the Guyanese population. Importantly, this informative case also highlights the utility of long-read SMRT sequencing to map nucleotide breakpoints of clinically relevant structural variants.

npj Genomic Medicine (2018)3:3; doi:10.1038/s41525-017-0042-3

INTRODUCTION

Bardet–Biedl syndrome (BBS) is a rare genetic disorder characterized by rod-cone dystrophy, truncal obesity, postaxial polydactyly, hypogonadism/genital anomalies, variable intellectual disability, and renal abnormalities. Secondary features can include hepatic fibrosis, diabetes mellitus, cognitive deficits, facial dysmorphism, short stature, and other pleiotropic congenital abnormalities.^{1,2} Variable expression of primary and secondary features is common, which is due, in part, to locus heterogeneity, yet intrafamilial clinical variability is also observed in some BBS cases.³ The mode of BBS inheritance is predominantly autosomal recessive; however, a multi-allelic inheritance pattern has been suggested for some BBS families.^{4,5}

A clinical diagnosis of BBS is based on the presence of primary and secondary clinical features;⁶ however, the recent availability of multi-gene sequencing panels has facilitated molecular diagnosis, estimation of recurrence risk, and targeted mutation testing for extended family members. To date, 20 genes involved in multi-subunit cilia assembly and function have been implicated in BBS,⁷ and the spectrum of pathogenic mutations in these genes

includes loss-of-function missense, nonsense, and structural variants. Herein, we report a Guyanese proband with a homozygous *BBS9* deletion encompassed by a 17.5 Mb region of homozygosity on chromosome 7p14.2–p21.1. The identical heterozygous *BBS9* deletions and shared haplotypes in the parents suggests that this pathogenic aberration may be a founder mutation in the Guyanese population.

RESULTS

Postnatal clinical evaluation

At 12 months of age, the male proband had a history of excessive weight gain despite no reported excess in feeding, prompting a referral to Medical Genetics for evaluation of an overgrowth syndrome. He was the second child of healthy, reportedly non-consanguineous Guyanese parents. At 14 months, his weight was 19.16 kg (100th pct, +5.8 SD), his length was 84.4 cm (99th pct, +2.29 SD), his head circumference was 52 cm (100th pct, +4.06 SD), and his BMI was 26.9 kg/m². Examination revealed a round face, low-set ears with fleshy lobes, a right ear pit (Fig. 1), a 2 × 1

¹Department of Genetics and Genomic Sciences, Icahn School of Medicine at Mount Sinai, New York, NY 10029, USA; ²Sema4, a Mount Sinai Venture, Stamford, CT 06902, USA and ³Icahn Institute for Genomics and Multiscale Biology, Icahn School of Medicine at Mount Sinai, New York, NY 10029, USA

Correspondence: Ethylin Wang Jabs (ethylin.jabs@mssm.edu) or Stuart A. Scott (stuart.scott@mssm.edu)

⁴Present address: Sanford Genetics and Genomic Laboratory, Sioux Falls, SD 57105, USA

⁵Present address: Department of Pediatrics, Division of Medical Genetics, Northwell Health, Lake Success, NY 11020, USA

⁶Present address: Division of Cytogenetics and Molecular Pathology, Donald and Barbara Zucker School of Medicine at Hofstra Northwell, Northwell Health Laboratories, Lake Success, NY 11042, USA

Received: 27 October 2017 Revised: 22 November 2017 Accepted: 5 December 2017

Published online: 22 January 2018

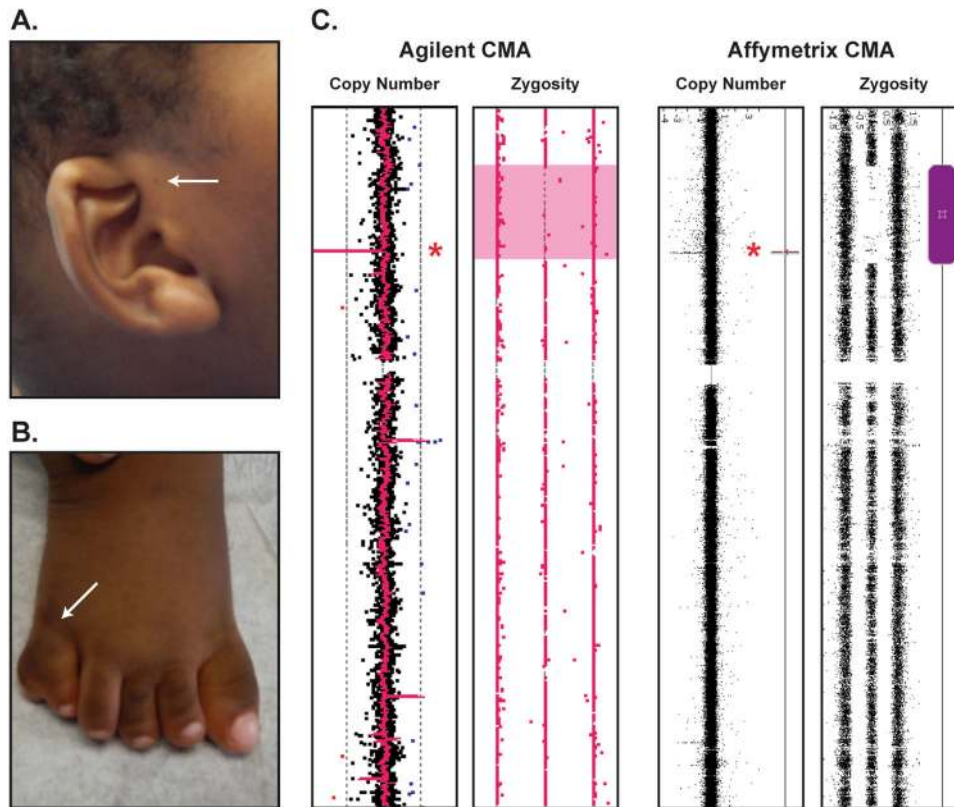


Fig. 1 Clinical and genetic diagnosis of Bardet-Biedl syndrome. Clinical evaluation of a 14-month-old proband revealed features suggestive of BBS, including low-set ears and a right ear pit (arrow) (a), and postaxial polydactyly on the right foot (arrow) (b). Analysis of the patient specimen on the Agilent 4 × 180 CGH + SNP array (c, left panel) detected a single region of homozygosity at chromosome 7p14.2–p21.1. A homozygous deletion (indicated by an asterisk) of the 5' region of *BBS9* was nested within the region of homozygosity at 7p14.3. Analysis of the proband DNA with the higher-resolution Affymetrix CytoScan HD array (c, right panel) confirmed these results and further refined the deletion breakpoints

cm café-au-lait spot on the right chest, and postaxial polydactyly on his right foot (Fig. 1). His genitalia appeared normal, partially hidden in a large fat pad, with a stretched penile length of 3.7 cm (25–50th pct). He demonstrated marked axial and appendicular hypotonia, and had significant difficulties in visual tracking. He started sitting up at 10 months but was unable to pull up to stand at 14 months. Although he could babble, he had not yet said his first word. His daily dietary intake consisted mostly of fruits, vegetables, and 12 ounces of breast milk, as carbohydrates were restricted in an attempt to limit weight gain. His comprehensive metabolic panels, including glucose and endocrine workup (TSH, T4-free thyroxine, T4 total, T3 total, IGF, and IGFBP-3), were normal. At 2 years, his cholesterol (214 mg/dl) and LDL (157 mg/dl) were elevated with his highest hemoglobin A1C at 5.7%. At 3 years, his vitamin D, 25-OH was low at 26 ng/ml. Kidney ultrasonography was normal at the time of evaluation; however, a 1-year follow-up was recommended to monitor for renal cysts and calyceal diverticula, which are common features among young children with BBS.^{8,9} Ophthalmologic examination showed small amplitude vertical nystagmus in association with reduced photopic and scotopic ERGs and normal fundi. Echocardiogram revealed a structurally normal heart with normal biventricular function. Auditory brain response revealed slight hearing loss at 500 Hz with normalization at higher frequencies. Based on these findings, a clinical diagnosis of BBS was made according to established criteria.⁵

Clinical cytogenomic and molecular genetic analyses

Cytogenetic analysis of the proband revealed a normal male karyotype in peripheral blood lymphocytes; however,

chromosomal microarray (CMA) testing detected a homozygous 7p14.3 deletion (minimum size: 43.0 kb; maximum size: 119.6 kb) nested within a 17.5 Mb region of homozygosity at chromosome 7p14.2–p21.1 (Fig. 1). The molecular karyotype was reported as: arr [hg19] 7p21.1p14.2(18969411_36497446)×2 hmz,7p14.3(33150658_33193639)×0. The minimum-sized deletion included exons 1–3 of *BBS9*, which is a known Mendelian disease gene implicated in autosomal recessive BBS. The homozygous *BBS9* deletion was independently confirmed by a clinical ciliopathy sequencing panel, which reported a homozygous loss of exons 2–4 of *BBS9*. Exon 1 of *BBS9* was not amenable to copy number analysis by sequencing due to the high GC content of this 5' exon.

Analysis of parental DNA by CMA testing indicated that both parents were heterozygous carriers of the identical 7p14.3 deletion. The absence of additional regions of homozygosity throughout the proband's genome supported the denial of known consanguinity.

Deletion breakpoint identification

Based on the probe spacing of the Agilent CMA platform, the identified homozygous deletion potentially included the neighboring retinitis pigmentosa gene, *RP9* (Fig. 2),¹⁰ which prompted additional studies to refine the deletion breakpoints to determine the risk of this condition in the proband and his carrier parents. As such, a series of PCR primers were designed to amplify specific regions between the minimum and maximum CMA deletion breakpoints. As illustrated in Fig. 2, only primer sets 1, 2, 3, and 9 successfully amplified in the proband, indicating that primer sets 4–8 were within the homozygous deletion. These results

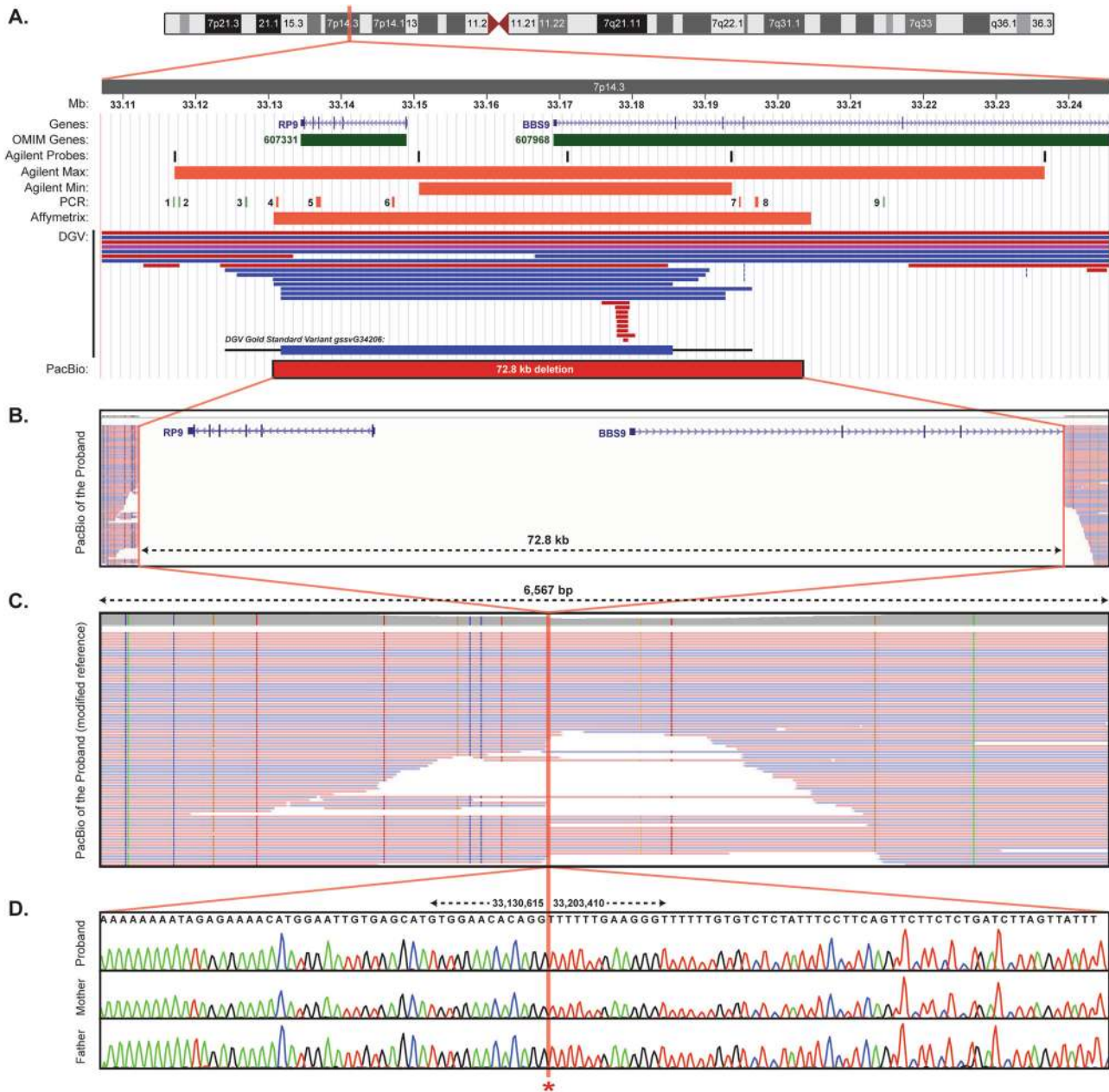


Fig. 2 Deletion breakpoint identification. The chromosome 7p14.3 genomic region is illustrated with tracks for the proband chromosomal microarray (CMA) results, genomic PCR mapping amplicon locations (1–9; green: amplified; red: did not amplify), and copy number variants detected among healthy individuals in the Database of Genomic Variants (DGV; blue: duplication; red: deletion) (a). Unambiguous breakpoint mapping was performed by long-read single molecule real-time (SMRT) sequencing (PacBio) of long-range PCR products that amplified across the deleted interval in the proband (b). These SMRT sequencing data were also aligned to a modified human genome reference that excluded the identified 72.8 kb deletion (chr7:33130616–33203409) (c), confirming that there were no other sequence alterations at the breakpoint locations. The precise deletion breakpoints were subsequently confirmed in the proband and both carrier parents by Sanger sequencing of the long-range PCR amplicons (d)

suggested that the entire *RP9* gene was included within the deletion, in addition to exons 1–4 of *BBS9*, and narrowed the distal and proximal deletion breakpoints.

Higher-resolution Affymetrix CMA testing of the proband further refined the deletion breakpoints (Fig. 2). Fine mapping was subsequently accomplished by long-range PCR across the narrowed breakpoints and subjecting the overlapping ~5.3–6 kb amplicons to third-generation single molecule real-time (SMRT) sequencing. Long-read SMRT sequencing, and confirmatory Sanger sequencing, identified the precise nucleotide breakpoints in the proband and heterozygous parents, which encompassed 72.8 kb of

chr7:33,130,616–33,203,409 (hg19) (Fig. 2). The flanking sequence of the breakpoints did not reveal any repetitive or homologous elements; however, interrogation of the Database of Genomic Variants (DGV; <https://dgv.tcag.ca>) revealed that the reciprocal duplication of this deletion (DGV Gold Standard Variant gssvG34206) is found in the general population at a frequency of 0.27% (Fig. 2).

DISCUSSION

The *BBS9* gene encodes PTHB1, which is an essential component of the BBSome cilia trafficking protein complex.¹¹ Although the

specific function of PTHB1 is currently unclear, knockdown of *BBS9* expression in zebrafish decreases cilia density and length, and causes brain and eye abnormalities that are rescued by ectopic expression of human *BBS9* mRNA.¹² Since the initial *BBS9* mutation families were identified,¹³ it is estimated that *BBS9* accounts for ~6% of all BBS cases.^{1,9} The spectrum of reported *BBS9* mutations suggests that loss-of-function single-nucleotide variants (e.g., splicing, nonsense, and frameshifts) and larger gene-disrupting copy number variants (CNVs) are pathogenic. To date, deletions of exons 8–9, exon 9, and exon 31 of *BBS9* have been identified in probands with BBS.^{14,15} Our study extends the *BBS9* mutation landscape to now include a 72.8 kb deletion of exons 1–4 and the neighboring *RP9*.

Notably, ophthalmologic evaluation of the proband and his parents did not detect evidence of retinitis pigmentosa to date, suggesting that *RP9* variants may present with later onset, have incomplete penetrance, or that the *RP9* missense mutations (c.410A > T; p.His137Leu and c.509A > G; p.Asp170Gly) previously reported in a single family may actually be benign rare variants.¹⁰ Of these two reported variants, only c.509A > G (rs104894039) was observed in the Genome Aggregation Database (gnomAD; <http://gnomad.broadinstitute.org/>), but with a very rare minor allele frequency (0.000065). Of note, a frameshift *RP9* variant has also been reported among individuals with hereditary retinal dystrophy (c.664delT; p.Ter222Aspfs; rs553265417); however, its appreciable European (non-Finnish) allele frequency in gnomAD (0.01083) suggests that it is likely benign.¹⁶ Given the uncertain clinical significance of homozygous or heterozygous loss of *RP9*, continued ophthalmologic evaluation of the proband and parents is planned.

The 7p14.3 deletion breakpoints were identified by an innovative long-read SMRT sequencing strategy, which revealed a low-copy repeat/LTR and a LINE element at the distal and proximal breakpoints, respectively. The absence of sequence homology at both breakpoints excluded non-allelic homologous recombination and microhomology-mediated break-induced repair as mechanisms of CNV formation. However, analysis of the deleted region revealed several inverted repeats with homology ranging from 74 to 100%. Inverted repeats can form hairpins and cruciform structures, and the resultant fork-stalling and DNA breakage can lead to non-homologous end joining.¹⁷ As noted above, the DGV indicates that the reciprocal 7p14.3 duplication occurs in the general population (0.27% frequency), which supports the hypothesis that a predisposition for rearrangement exists at 7p14.3 due to local genomic architecture.

Interestingly, the homozygous 7p14.3 deletion was encompassed by a single 17.5 Mb region of homozygosity at 7p14.2–p21.1. Familial consanguinity was denied; however, both parents indicated they were from the small Mahaicony region of Guyana. Guyana is one of the smallest countries in mainland South America, but is ethnically diverse with its population being comprised of Indian, African, and Amerindian ancestry. Of note, Guyanese founder mutations have previously been reported, including a *LIPH* mutation on chromosome 3q27.2 that results in autosomal recessive woolly hair/hypotrichosis.¹⁸

In conclusion, we describe a homozygous *BBS9* deletion detected in a BBS proband from a Guyanese family, with precise breakpoints delineated by long-read SMRT sequencing. Long-read SMRT sequencing also determined that the deletion encompassed the neighboring retinitis pigmentosa gene, *RP9*; however, the clinical significance of this was considered uncertain. Importantly, the identification of this shared *BBS9* deletion haplotype in the parents suggests that further studies are warranted to determine the allele frequency and incidence of BBS in the Guyanese population.

METHODS

Clinical evaluation

Clinical evaluation was performed at the Genetics Clinic at the Icahn School of Medicine at Mount Sinai by genetic counselors and clinical geneticists (L. P. and E.W.J.). The family provided written informed consent for Icahn School of Medicine at Mount Sinai Institutional Review Board-approved research participation and publication of photographs.

Clinical cytogenetic and molecular genetic testing

Clinical cytogenomic testing included peripheral blood G-banded chromosome and CMA analysis performed at Mount Sinai Genomics Inc. (DBA Sema4; previously known as the Mount Sinai Genetic Testing Laboratory). DNA from the proband was tested on the SurePrint G3 ISCA CGH+SNP 4 × 180K array (Agilent Technologies, Santa Clara, CA), as per the manufacturer's instructions and as previously described.^{19,20} Higher-resolution CMA testing of the proband on the CytoScan[®] HD platform (Affymetrix, Santa Clara, CA) was performed per the manufacturer's instructions and as previously reported.²⁰

Clinical molecular testing included a 55-gene ciliopathy sequencing panel (Supplemental Table 1) performed at Invitae (San Francisco, CA). Enrichment and sequencing was restricted to coding regions and 10 bp of flanking intronic sequence at a minimum depth of 50×. Exonic deletions and duplications were assessed using a proprietary algorithm that compared read depth of target sequences in the proband to internal control samples.

BBS9 breakpoint identification

Genomic DNA PCR amplification: The deletion breakpoints were interrogated by PCR amplification of genomic DNA using a series of primers designed to generate amplicons at specific regions between the minimum and maximum deletion coordinates estimated by CMA testing (Supplemental Table 2).

Long-read SMRT sequencing: Long-range PCR amplification across the identified breakpoint regions was accomplished using primers targeted to unique DNA sequences flanking the approximated deletion coordinates, and these amplicons were subjected to SMRTbell library construction and long-read SMRT sequencing (Pacific Biosciences, Menlo Park, CA). Long-range PCR reactions were performed in 50 µl containing ~100 ng of DNA, 1× LA PCR buffer II (TaKaRa), 0.4 µM of barcoded forward and reverse primers (Supplemental Table 2), 0.4 mM dNTPs, 1 µl DMSO, and 2.5 units of TaKaRa LA Taq HS. Amplification consisted of an initial denaturation step at 95 °C for 5 min followed by 10 amplification cycles (95 °C for 30 s, 61 °C for 30 s, and 72 °C for 10 min), another 20 amplification cycles (95 °C for 30 s, 56 °C for 30 s, and 72 °C for 10 min), and a final extension at 72 °C for 15 min. All PCR amplicons were purified, quantified, pooled, sequenced (P6-C4 PacBio protocol), and analyzed as previously described.²¹

Data availability

The long-read SMRT sequencing FASTQ data are available from the NCBI Sequence Read Archive (SRA) using the SRP125431 experiment identifier: <https://www.ncbi.nlm.nih.gov/sra/SRP125431> [accn].

ACKNOWLEDGEMENTS

The authors would like to thank the proband and family for supporting publication of this case report. In addition, the authors thank Affymetrix (Thermo Fisher Scientific) for supporting the CMA testing with the Affymetrix CytoScan HD array. This study was supported, in part, by Mount Sinai Genomics, Inc. (DBA Sema4) at the Icahn School of Medicine at Mount Sinai.

AUTHOR CONTRIBUTIONS

J.R. and S.A.S. conceived the case report, reviewed the literature, analyzed and interpreted all data, and drafted and revised the manuscript; L.P. and E.W.J. conceived the case report, oversaw the clinical workup, analyzed and interpreted all data, and revised the manuscript; W.Q., R.S., Y.Y., L.S., W.A.K., R.S., N.C., A.B., and L.E. contributed data, analyzed and interpreted all data, and revised the manuscript.

ADDITIONAL INFORMATION

Supplementary information accompanies the paper on the *npj Genomic Medicine* website (<https://doi.org/10.1038/s41525-017-0042-3>).

Competing interests: The authors declare no competing financial interests.

Publisher's note: Springer Nature remains neutral with regard to jurisdictional claims in published maps and institutional affiliations.

REFERENCES

1. Forsythe, E. & Beales, P. L. in *GeneReviews(R)* (eds Pagon, R. A. et al.) [Internet]. Seattle (WA) (1993).
2. Khan, S. A. et al. Genetics of human Bardet-Biedl syndrome, an updates. *Clin. Genet.* **90**, 3–15 (2016).
3. Suspitsin, E. N. & Imyanitov, E. N. Bardet-Biedl syndrome. *Mol. Syndromol.* **7**, 62–71 (2016).
4. Gropman, A. L. & Adams, D. R. Atypical patterns of inheritance. *Semin. Pediatr. Neurol.* **14**, 34–45 (2007).
5. Katsanis, N. The oligogenic properties of Bardet-Biedl syndrome. *Hum. Mol. Genet.* **13**, R65–R71 (2004).
6. Beales, P. L., Elcioglu, N., Woolf, A. S., Parker, D. & Flinter, F. A. New criteria for improved diagnosis of Bardet-Biedl syndrome: results of a population survey. *J. Med. Genet.* **36**, 437–446 (1999).
7. Wei, Q. et al. The BBSome controls IFT assembly and turnaround in cilia. *Nat. Cell. Biol.* **14**, 950–957 (2012).
8. M'Hamdi, O., Ouertani, I. & Chaabouni-Bouhamed, H. Update on the genetics of Bardet-Biedl syndrome. *Mol. Syndromol.* **5**, 51–56 (2014).
9. Daniels, A. B. et al. Genotype-phenotype correlations in Bardet-Biedl syndrome. *Arch. Ophthalmol.* **130**, 901–907 (2012).
10. Keen, T. J. et al. Mutations in a protein target of the Pim-1 kinase associated with the RP9 form of autosomal dominant retinitis pigmentosa. *Eur. J. Hum. Genet.* **10**, 245–249 (2002).
11. Jin, H. et al. The conserved Bardet-Biedl syndrome proteins assemble a coat that traffics membrane proteins to cilia. *Cell* **141**, 1208–1219 (2010).
12. Veleri, S. et al. Knockdown of Bardet-Biedl syndrome gene *BBS9/PTHB1* leads to cilia defects. *PLoS ONE* **7**, e34389 (2012).
13. Nishimura, D. Y. et al. Comparative genomics and gene expression analysis identifies *BBS9*, a new Bardet-Biedl syndrome gene. *Am. J. Hum. Genet.* **77**, 1021–1033 (2005).

14. Hjortshoj, T. D. et al. Bardet-Biedl syndrome in Denmark—report of 13 novel sequence variations in six genes. *Hum. Mutat.* **31**, 429–436 (2010).
15. Muller, J. et al. Identification of 28 novel mutations in the Bardet-Biedl syndrome genes: the burden of private mutations in an extensively heterogeneous disease. *Hum. Genet.* **127**, 583–593 (2010).
16. Glockle, N. et al. Panel-based next generation sequencing as a reliable and efficient technique to detect mutations in unselected patients with retinal dystrophies. *Eur. J. Hum. Genet.* **22**, 99–104 (2014).
17. Hastings, P. J., Lupski, J. R., Rosenberg, S. M. & Ira, G. Mechanisms of change in gene copy number. *Nat. Rev. Genet.* **10**, 551–564 (2009).
18. Shimomura, Y. et al. Founder mutations in the lipase *h* gene in families with autosomal recessive woolly hair/hypotrichosis. *J. Invest. Dermatol.* **129**, 1927–1934 (2009).
19. Scott, S. A. et al. Detection of low-level mosaicism and placental mosaicism by oligonucleotide array comparative genomic hybridization. *Genet. Med.* **12**, 85–92 (2010).
20. Reiner, J. et al. Chromosomal microarray detection of constitutional copy number variation using saliva DNA. *J. Mol. Diagn.* **19**, 397–403 (2017).
21. Qiao, W. et al. Long-read single molecule real-time full gene sequencing of cytochrome *P450-2D6*. *Hum. Mutat.* **37**, 315–323 (2016).



Open Access This article is licensed under a Creative Commons Attribution 4.0 International License, which permits use, sharing, adaptation, distribution and reproduction in any medium or format, as long as you give appropriate credit to the original author(s) and the source, provide a link to the Creative Commons license, and indicate if changes were made. The images or other third party material in this article are included in the article's Creative Commons license, unless indicated otherwise in a credit line to the material. If material is not included in the article's Creative Commons license and your intended use is not permitted by statutory regulation or exceeds the permitted use, you will need to obtain permission directly from the copyright holder. To view a copy of this license, visit <http://creativecommons.org/licenses/by/4.0/>.

© The Author(s) 2018